2025 IEEE/SICE International Symposium on System Integration (SII)
January 21-24, 2025, Munich, Germany

Stiffness and Strength Changes of 3D Printed Parts due to Bonding

Rintaro MATSUSHITA and Yusuke OTA

Abstract— **3D printed parts have anisotropic characteristics depending on the infill structure, and strength changes with infill rate. Recently, some researches have being conducted to elucidate their characteristics, and it is expected that 3D printed parts will be used as robot parts. However, since the size of the 3D printed parts depends on the size of the printers. It has been required to combine to make 3D printed parts. There are few strength evaluations that consider the combination of 3D printed parts. In this study, three-point bending experiments were conducted on 3D printed parts when two or more parts were adhered as one assembled 3D printed component, and the changes in strength and stiffness were confirmed to compare with non-bonded parts. In addition, experiments were also conducted for different bonded shapes and infill structures. As a result, the bonded parts exhibited 0.73 times the strength of the non-bonded parts, with no significant change in stiffness. And it was also shown that the strength changes depending on the bonding shape. Furthermore, the strength of the bond also showed increases depending on the infill structure and the infill rate.**

I. Introduction

The purpose of this study is to evaluate changes in strength and stiffness due to bonding. 3D printed parts are expected to be used in wide range of fields. The strength and printing accuracy of 3D printed parts have been investigated [1]-[4]. Recent studies have shown that 3D printed parts can be used as robotic parts [3]-[7]. However, the size of 3D printed parts that can be produced is limited by the size of the 3D printer. Therefore, there are problems when printing large robot parts, since it requires large and expensive 3D printers. New methodologies and their research to bond several 3D printed parts are now on going in order to make large 3D printed parts with bonding [8]. We have thought that filament material could be used as an adhesion, and that it would be possible to combine several parts without fitting them together. In this study, we placed the 3D printed parts to be modeled on the software in a way that they slightly overlap. In addition, based on the expansion of the size of the 3D printed parts during printing [9], the overlap distance between the two parts was adjusted in the software to clarify whether there was any change in strength and stiffness. And experiments were also conducted on test rods with different bond shapes and infill structures to confirm the change in strength and stiffness.

All authors are with the Department of the Advanced Robotics, Chiba Institute of Technology, 2-17-1 Tsudanuma, Narashino, Chiba 257-0016JAPAN (e-mail: s20C1107RA@s.chibakoudai.jp).

II. Strength and Stiffness Changes due to Bond

To evaluate the strength and stiffness of the bonded shapes in this study, a three-point bending experiments have been conducted and the following aspects are addressed.

- Laminate direction and load direction: Evaluate the strength and stiffness of the bonded shapes. It is necessary to measure the change in strength and stiffness of the 3D-printed parts when formed as a single part. The anisotropy of 3D-printed parts is compared in three-point bending experiments using three different patterns that is considered the laminated and loading directions. This value is used as a standard value for comparison with the case of bonded. (section III-A)
- Strength and stiffness in different bonded distance: To confirm the change in strength and stiffness when 3D printed parts are bonded together, it is confirmed the change in strength and stiffness depending on the overlap distance between the 3D printed parts which is bonded. (section III-B)
- Bonded shapes: Seven different test rods were prepared and tested for each bonded shape, considering the laminated and loading direction. (section III-C)
- Infill structure: The infill structure design must be important to develop the lighter parts with strong stiffness. This is because the infill structure and infill rate within the 3D printer can be changed to create lightweight and rigid parts [1]. Based on these considerations, we will confirm whether the strength and stiffness of the bonded parts change depending on the infill structure. (section III-D)

We have fabricated experimental parts using the Markforged Mark Two as a 3D printer [10]. The 3D printed parts are made by Onyx™ [11], that is the nylon based material, and without continuous carbon fiber contains in this research. The printing method was Fused Deposition Modeling (FDM). We confirmed the actual change in strength of 3D printed parts due to bonding by referring to a three-point bending experiments [12].

Fig. 1 shows experimental setup and experimental coordinates. The three point bending experiments were conducted using the AIKOH motorized stand with a force gauge attached. The force gauge was applied to the center of the test rod (specimen by 3D printed parts) to measure the force, and the force gauge was moved at 10 mm/min in the Z-

axis direction. The moved distance was measured by CCD Laser Displacement Transducer (Keyence LK-G150).

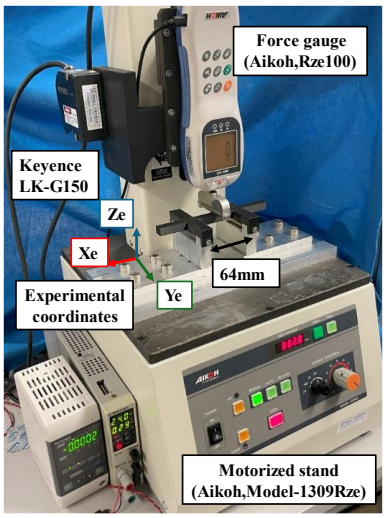

Figure 1. Three-point bending test machine

III. Strength and Stiffness Changes Due to Bonding

We performed three-point bending experiments to confirm the changes in strength and stiffness due to bonding.

A. Laminated Direction and Load Direction

To confirm the strength and stiffness of the 3D printed parts in the laminated and loading directions, three-point bending experiments were conducted. Two different laminated directions were used as the test rods. Figs. 2 and 3 show the coordinate system of the test rods used the experiments and the laminated direction of 3D printed part. The printed parts laminated in Zm-direction as shown in Fig. 2 is named "test rod A" and laminated in Ym-direction as shown Fig. 3 is named "test rod B". The two test rods were modeled using 3D-CAD (Autodesk Inventor) and consist of 10×10×150 mm. The infill structure of both test rods was solid, that infill rate was 100%. Test rods with a laminated pitch of 0.1 mm and a wall layer of 0.4 mm was used. The experiments were also performed by seven test rods which were printed once.

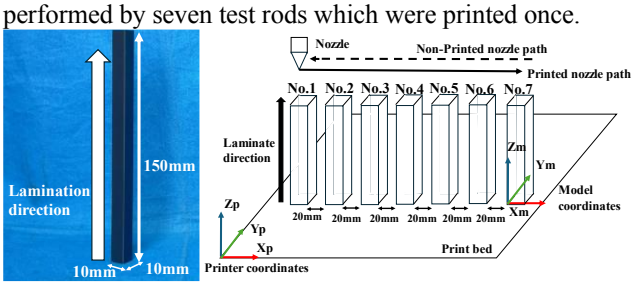

Figure 2. Test rod A printed placement

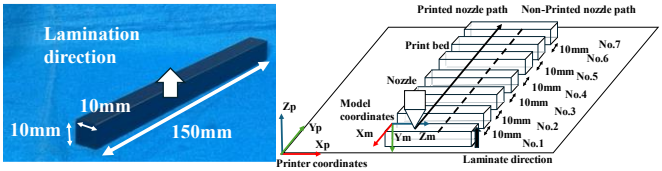

Figure 3. Test rod B printed placement

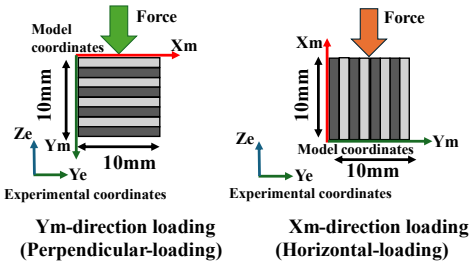

Figure 4. Force applications direction and laminated direction

Test rod A was loaded from one direction. This is because, infill of solid has isotropy characteristics so the interior shape does not change due to differences in the loading direction. Test rod B was loaded from the two directions shown in Fig. 4. The load perpendicular to the Print bed is referred to as "Ym-direction loading", and the load in the direction horizontal to the Print bed is "Xm-direction loading", shown in Fig. 4. Figs. 5 to 7 show the results of each of three-bending experiments.

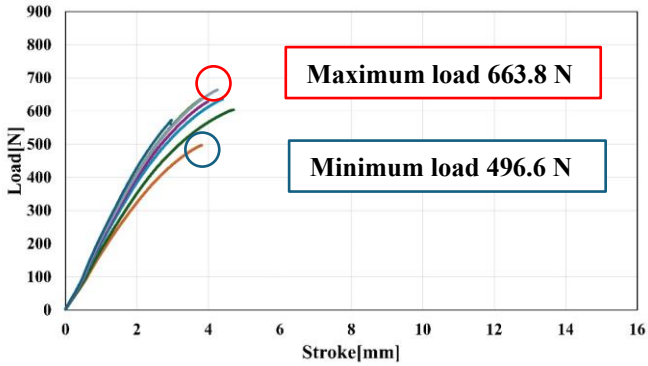

Figure 5. Loading result of Test rod A to Ym direction

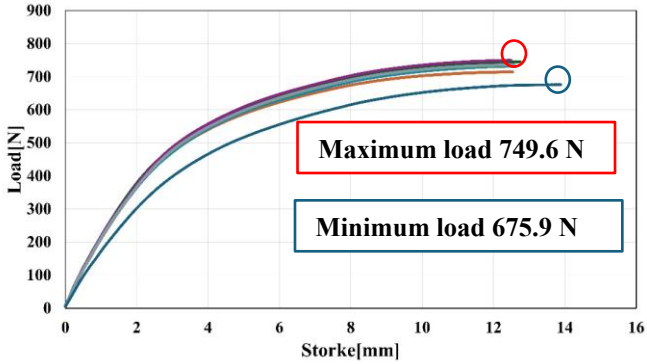

Figure 6. Loading result of Test rod B to Ym direction

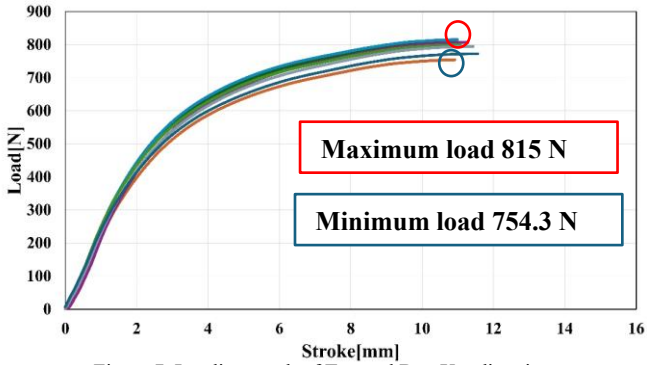

Figure 7. Loading result of Test rod B to Xm direction

Table I summarizes the average strength and stiffness values shown in Figs. 5 to 7. The stiffness values were calculated from the strength results obtained from the three-point bending experiments. The stiffness values were calculated from the slope values between 15% and 65% of the load, with load on the vertical axis and stroke on the horizontal axis, as shown in Figs. 5 to 7. Table I shows that the results of the three-point bending experiment confirmed the change in strength and stiffness values from the comparison of test rod A and B. Test rod B results in higher strength and lower stiffness compared with test rod A. The difference in the load direction of test rod B confirmed the change in strength and stiffness due to anisotropy. These results have a consistence with previous findings [1]. In the present study, these strength and stiffness values are used as standard values for comparison value for evaluation by bonding.

Table I. Variation of strength and stiffness by laminated direction and printing direction

Test rod pattern	average load[N]	average stiffness[N/mm]	average mass[g]
Test rod A	605.53	194.57	16.479
Test rod B load direction Ym	726.73	141.07	16.186
Test rod B load direction Xm	793.16	178.96	16.065

B. Strength and Stiffness for Difference Bonded Distance

To confirm the strength and stiffness of the 3D printed part bond, the test rod used in the previous experiment was divided into two 75×10×10 mm test rods. Fig. 8 shows the divide of the 3D printed parts, with the test rod placed on the left side as Part 1 and the test rod placed on the right side as Part 2. Fig. 8 shows the divide of the test rod in the case of test rod B (horizontal laminated), so that the 3D printed parts partially overlap and are bonded together. The bonding method used in this study is to bond 3D printed parts by placing them so that some of them overlap each other on the slicer software (IGER) for the 3D printer of Marktwo. It was found that the dimensions of 3D printed parts became larger than the designed values at the time of printing in previous studies [1]. Therefore, it was also verified in the case where 3D printed parts were placed and bonded without overlapping. Table II shows the overlap distance between the two test rods, the average mass of the test rods, and the average strength and stiffness values from three-point bending experiments. The mass, strength, and stiffness results are summarized as the average of the results from seven test rods. Negative overlap distances indicates that the test rods are divided from each other, and for zero overlap distances indicates the specimens are placed adjacent to each other. And then they were printed by their overlapped distances. The experiment was conducted with the Ym-direction loading. (perpendicular loading direction).

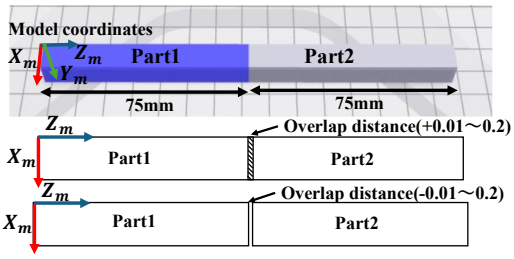

Figure 8. Bonded parts

Table II. Strength and stiffness at different overlap distances

overlap distance[mm]	average load[N]	average stiffness[N/mm]	average mass[g]
-0.2	424.74	150.49	16.650
-0.1	464.90	101.45	16.244
-0.05	518.03	131.71	16.440
-0.04	523.51	137.61	16.419
-0.03	524.04	126.56	16.503
-0.02	485.57	124.17	16.284
-0.01	541.66	142.05	16.476
0	504.04	130.61	16.386
0.01	619.37	180.49	16.352
0.02	543.93	151.80	16.182
0.03	552.51	167.60	16.337
0.04	502.51	121.37	16.231
0.05	524.27	120.39	16.151
0.1	566.77	151.62	16.258
0.2	556.63	124.55	16.397

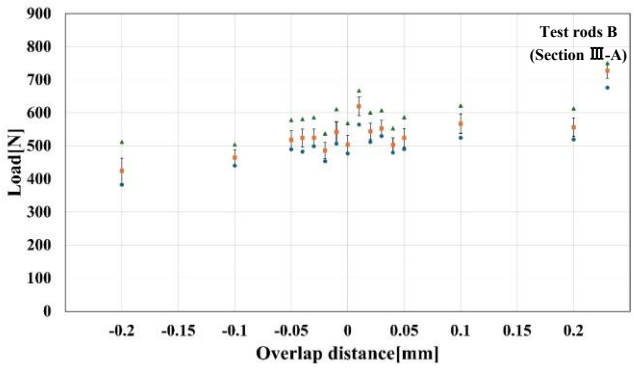

Figure 9. Strength change with bonding distance

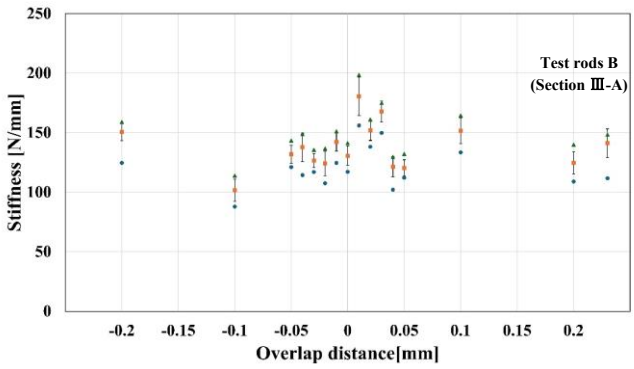

Figure 10. Stiffness changes with bonding distance

Figs. 9 and 10 show the change in strength and stiffness values. The results in Fig. 9 show that, compared to test rods B (Section III-A), which was printed as a single piece, the strength is 0.73 times greater when the two 3D printed parts are bonded in software at ±0.05mm. The results also show that when the overlap distance is -0.1 and -0.2 mm, the strength is 0.64 and 0.58 times lower, indicating a significant reduce in strength. From 0.1 and 0.2 mm when the overlap distance is increased, the values are 0.78 and 0.77 times higher, confirming that the increase in strength by increasing the overlap distance does not have a significant effect. Fig. 10 shows that there is little change in the stiffness value,

confirming that the strength of the joint surface decreases, but the stiffness value remains high.

C. *Bonded Shapes*

The characteristics of the change in strength and stiffness of the bond were confirmed. However, bonded strength and stiffness may be affected by the bonded shape. To test the performance of the strength and stiffness of different bonded shapes, 3D printed parts with two different bonded shapes were printed. Experiments were conducted in two different loading directions for all types of bonding shapes. The overlap distance was set to 0 mm in the software. Two shapes of bonding of 3D printed part and coordinate system are shown in Fig. 11.

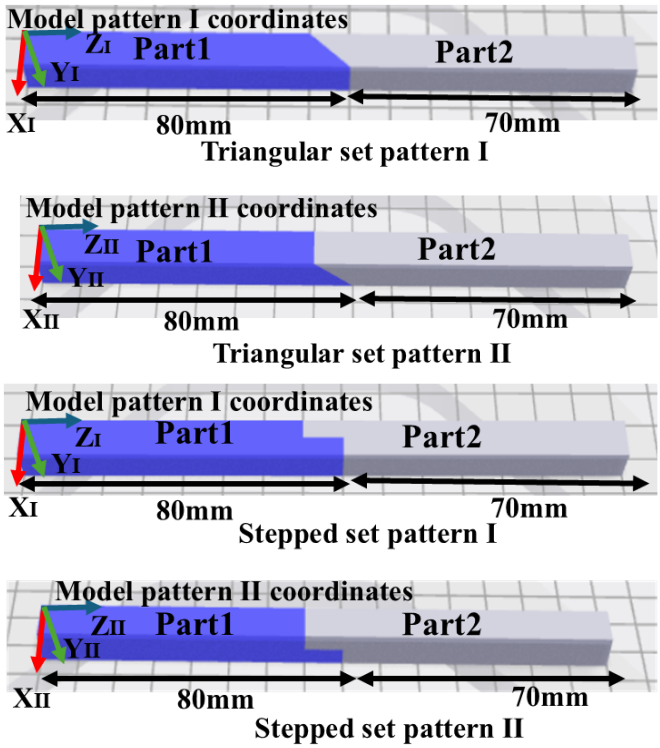

Figure 11. Bonded shapes and coordinate system

Figs. 12 and 13 show the experimental results of strength in load direction Y(I・II) and X(I・II). Figs. 14 and 15 show the experimental results of stiffness in direction Y(I・II) and X(I・II). From the three-points bending experiments result in Figs 12 and 13, the strength depends on bonded shape. According to Figs. 14 and 15, the stiffness value increases when a load is applied horizontal (X(I・II)-direction loading) to the print bed. Table III summarizes the average strength and stiffness values for Figs. 12 and 14. Table IV summarizes the average strength and stiffness values for Figs. 13 and 15. Fig. 16 shows the fracture shape and fracture surface of the 3D printed parts in Fig. 11. When comparing the fracture surfaces of the triangular and stepped set pattern, the triangular set pattern exhibited a smoother fracture surface, and the peeling phenomenon was observed.

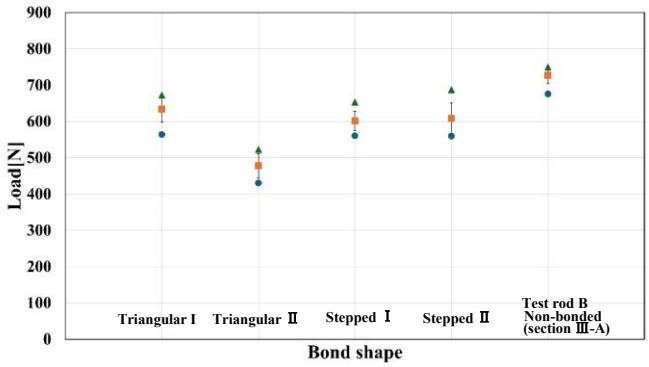

Figure 12. Strength in Y(I・II)-direction loading

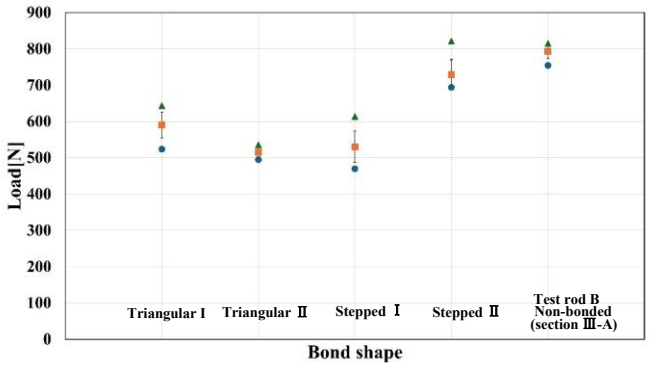

Figure 13. Strength in X(I・II)-direction loading

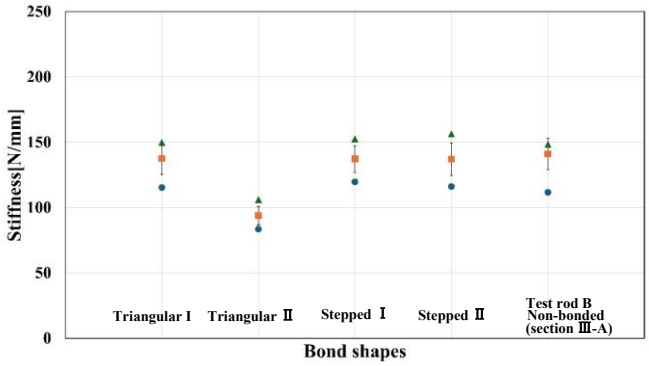

Figure 14. Stiffness in Y(I・II)-direction loading

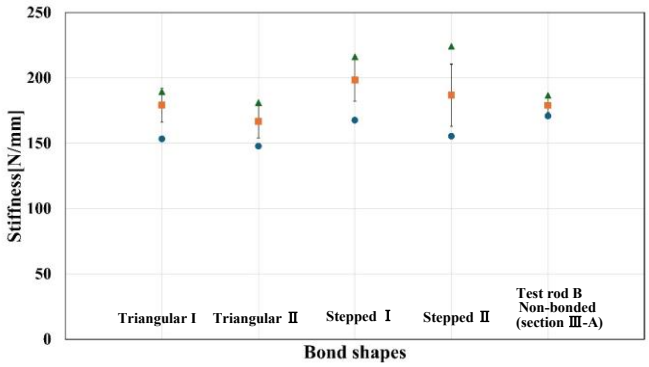

Figure 15. Stiffness in X(I・II)-direction loading

Table III. Y(Ⅰ・Ⅱ)-direction loading

Bond shape	Average load[N]	Average stiffness[N/mm]	Average mass[g]
Triangular set pattern Ⅰ	634.07	137.53	16.378
Triangular set pattern Ⅱ	477.71	93.83	15.856
Stepped set pattern Ⅰ	601.69	137.14	16.276
Stepped set pattern Ⅱ	608.24	137.04	16.384

Table IV. X(Ⅰ・Ⅱ)-direction loading

Bond shape	Average load[N]	Average stiffness[N/mm]	Average mass[g]
Triangular set pattern Ⅰ	590.07	179.12	16.395
Triangular set pattern Ⅱ	515.47	166.65	15.840
Stepped set pattern Ⅰ	530.01	198.34	16.241
Stepped set pattern Ⅱ	728.88	186.77	16.322

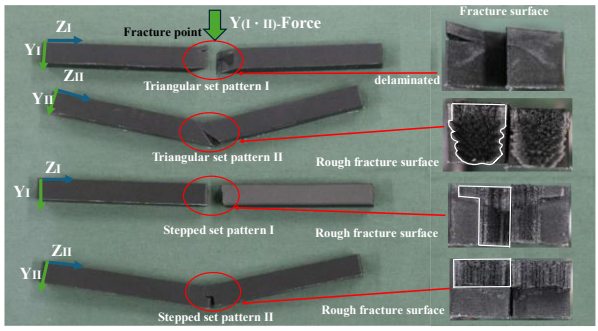

Y(Ⅰ・Ⅱ)-direction loading

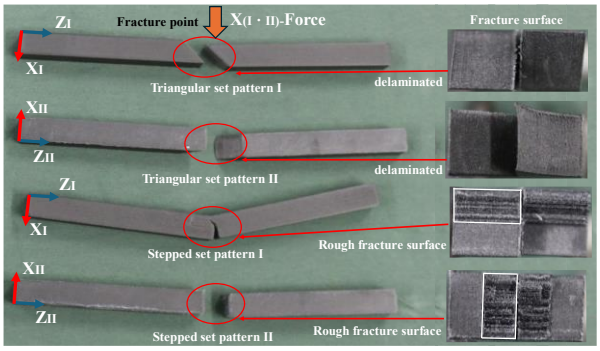

X(Ⅰ・Ⅱ)-direction loading

Figure 16. Fracture shape and fracture surface

Fig. 17 shows the experimental results for each bond shape for Y(Ⅰ・Ⅱ)-direction loading. The results are summarized by the highest load among the seven test rods printed. It can be shown from Fig. 17 that the strength of the bond remains higher than that of a linear bond (section Ⅲ-B), expect for the triangular set pattern Ⅱ.

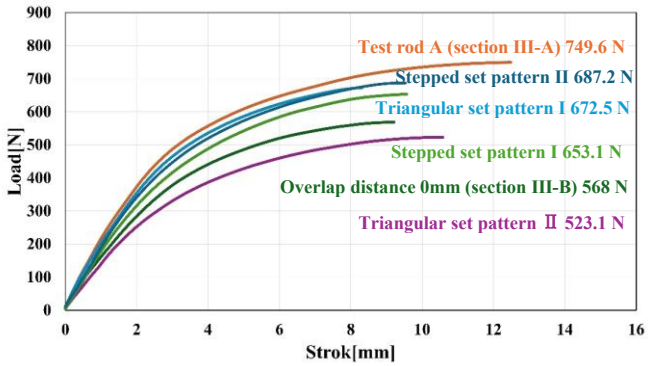

Figure 17. Strength comparison of different bond shapes

Changes in strength and stiffness when bonded in the height direction were also evaluated. Test rods of similar shapes were bonded in the height direction. Cube bond with an overlap distance of 0 mm (section III-B) were also performed for the height bond. Height bonding was performed by placing part 1 on the bottom and part 2 on the top as shown in Fig. 18. In consideration of the bonding shapes, two loading directions, Ym and Xm, are examined. The same experiment was performed on the specimens without bonding and used as the standard value.

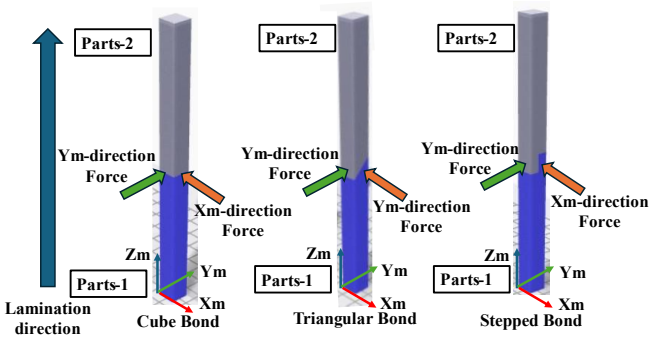

Figure 18. Applied force direction and bonding shapes in test rod A

The results of the bond in the height direction showed that the strength were 0.78 times higher in direction Ym and 0.92 times higher in direction Xm than the reference value. Triangular bonding confirmed that the strength were 0.50 times higher in direction Ym and 0.49 times higher in direction Xm than that of without bonding. In addition, the stiffness value is greater for the bonded in the height direction. It was also observed that the strength was significantly reduced in patterns that bonded at an angle to the laminated direction, such as the Triangular set pattern II in Fig. 11 and the Triangular Bond in Fig. 18.

Table V. Strength and stiffness change with height laminated

Bond shape and load direction	Average load[N]	Average stiffness[N/mm]	Average mass[g]
Cube (without bonding) Ym direction	605.53	194.57	16.479
Cube (without bonding) Xm direction	656.93	158.06	16.563
Cube bond Ym direction	473.46	213.12	16.554
Cube bond Xm direction	603.10	182.03	16.521
Triangular bond Ym direction	305.47	211.59	16.621
Triangular bond Xm direction	319.59	222.79	16.567
Stepped bond Ym direction	595.90	221.96	16.614
Stepped bond Xm direction	599.40	155.60	16.498

D. Infill Structure

Strength and stiffness would be also affected much with their infill structure, then these changes with bonding varying the infill structure and infill rate were also investigated. The bonded parts were the same shapes as in Section III-B, with an overlap distance of 0 mm and were arranged on the software so that the parts were adjacent to each other. Three-point bending tests were also conducted on a 10×10×150 mm one-piece specimen with 37% triangular infill. This value is used as a standard value for comparison with the case of bonded. The three-point bending results of the bonded test rods and test rods without bonding are summarized in Table VI.

Table VI. Change of strength and stiffness due to 37% triangular infill

Bond shape and load direction	Average load[N]	Average stiffness[N/mm]	Average mass[g]
Non bonding-Ym direciton	288.63	59.84	8.569
Non bonding-Xm direciton	326.21	106.38	8.468
Cube bonding-Ym direction	262.49	67.45	8.629
Cube bonding-Xm direction	371.13	119.60	8.671

In terms of the change in strength due to bonding, it was confirmed that higher strength was obtained in the Xm-direction loading. The strength in Ym-direction loading at the time of bonding is 0.91 times the standard value. It can be verified that the change is higher than the change relative to the standard value of the results of the bond at solid (SECTION III-B). Fig. 19 shows, that the bonding point of the two parts consist of the wall layer, that means a creating area has a 100% infill rate. This effect to increase the infill rate of the loaded part is thought to increase its strength. The results also indicate that the bonding methodology in 3D printing can be usefully fabricated to maintain their lightweight with relatively high stiffness. From these results, it is necessary to determine how much the strength and stiffness of the bond should change as the infill rate is increased.

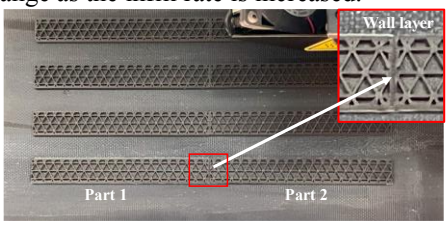

Figure 19. Infill structure and bond points during printing

IV. Conclusion

In this study, several experiments have been conducted to clarify the strength and stiffness characteristics of 3D printed parts by bonding. In the experiments, the specimens had been printed by 3D printer to evaluate their strength and stiffness by three-point bending test machine. First, three-point bending experiments were conducted on the anisotropy of the properties of 3D printed parts to confirm the change in strength and stiffness due to anisotropy. Obtained results were used as a standard value to compare the strength stiffness when bonded. Next, the differences depending on the bonding distance has been quantitively evaluated. If the overlap distance is within ±0.05mm, the strength decreases by 0.73, and the stiffness value does not change. Then, differences in strength and stiffness due to the shape of the bonding were confirmed. From the experimental results, the triangular and stepped bond shapes showed higher strength than cube bonds. These results also indicate that the shape for bonding is more important than overlapping distance with respect to strength. High stiffness was observed in height direction bonding. It has also been confirmed that the strength change is significantly lower depending on the direction of triangular bonding. Bonding shapes with difficulty of delamination would be our future research subjects. Finally, it is confirmed the bond strength and stiffness for different infill structure. It is evaluated strength and stiffness by bonds of specimens with different infill structure and infill rate, changed from 100% solid infill to 37% triangular infill. When bonded at 37% triangular infill, the bonds maintained higher strength and stiffness when compared to the one-piece printing at 37% triangular infill.

In our future work for the strength and stiffness evaluation by bonding, we will increase the number of samples for each condition to accumulate more reliable experimental data. And, propose the method for creating printings that can be allows for bonding and creating large parts in practical robot design actually Robot design.

Acknowledgment

This research was subsidized by New Energy and Industrial Technology Development Organization (NEDO) under project JPNP20016. This paper is an achievement of joint research with and is jointly owned copyrighted material of ROBOT Industrial Basic Technology Collaborative Innovation Partnership. We thank Prof. Gen Endo (Institute of Science Tokyo), Prof. Naoyuki Takesue (Tokyo Metropolitan University), and Prof. Takeshi Takaki (Hiroshima University) for their valuable comments and discussion.

References

[1] Yusuke OTA, Ryuichi SHINA, Koki KATO and Rintaro MATSUSHITA “Geometric Shape Accuracy and Hygroscopic Characteristics of a 3D-printed Part” 2023 IEEE/SICE International Symposium on System Integration (SII), Atlanta, GA, USA, 2023, pp. 531-536.

[2] R. Matsushita and Y. Ota, "Size and Toughness Changes of 3D Printed Parts Due to Hygroscopic Characteristics," *2024 IEEE/SICE International Symposium on System Integration (SII),* Ha Long, Vietnam, 2024, pp. 1524-1530

[3] Hiroki Kanazawa, Hiroyuki Nabae, Koichi Suzumori, and Gen Endo “Empirical Study for 3D-Printed Robot Design: Dimensional Accuracy of a Hole and Proposal of a New Shaft-Fastening Method” 2022IEEE/SICE International Symposium on System Integration (SII), Narvik, Norway, 2022, pp. 633-639.

[4] K. Osawa and G. Endo, "Does Thin-Walled Metal Pipe Insertion Increase the Bending Strength of 3D Printed Parts?," *2024 IEEE/SICE International Symposium on System Integration (SII),* Ha Long, Vietnam, 2024, pp. 585-591

[5] T. Yoshida, G. Endo, A. Okubo and H. Nabae, "Experimental Evaluation of a Quasi-direct-drive Actuator with a 3D-printed Planetary Gear Reducer," *2023 IEEE/SICE International Symposium on System Integration (SII)*, Atlanta, GA, USA, 2023, pp. 1-6.

[6] H. Satake and N. Takesue, "Comparison of Characteristics of Cycloidal Gear Reducer Using Metal, Plastic and 3D Printed Parts," *2024 IEEE/SICE International Symposium on System Integration (SII),* Ha Long, Vietnam, 2024, pp. 1531-1536.

[7] Y. Bao and T. Takaki, "Influence of 3D Printing Filling Density on Vibration Characteristics of Robot Structure," *2024 IEEE/SICE International Symposium on System Integration (SII)*, Ha Long, Vietnam, 2024, pp. 598-603

[8] N Kanai, H Nabae, and G Endo,” Robot Mechanical Parts Made by 3D Printers for Industrial Applications”. -Report 9: Proposal of 3D Printed Parts Joining Method for Large-Size Parts-“ROBOMECH, 1P1-P04, 2024,Utsunomiya, Tochigi.

[9] T Takaki, “Fastening of plastic parts produced by fused-deposition-modeling 3D-printer with machine key” “ROBOMECH, 1A1-I16,2023, Nagoya, Aichi.

[10] https://www-objects.markforged.com/craft/3d_printers_detail/mark-two/F-PR-2027.pdf

[11] https://3dprinter.co.jp/cms3d/wp-content/uploads/2024/07/Markforged_CompositesV5_ja.pdf

[12] Japan Industrial Standards JIS K 7171